The Journal of Chemical Physics

RAPID COMMUNICATION | AUGUST 02 2012

Communication: Effect of the orbital-overlap dependence in the meta generalized gradient approximation FREE

Jianwei Sun; Bing Xiao; Adrienn Ruzsinszky

J. Chem. Phys. 137, 051101 (2012)
https://doi.org/10.1063/1.4742312

AIP Publishing

Communication: Effect of the orbital-overlap dependence in the meta generalized gradient approximation

Jianwei Sun, Bing Xiao, and Adrienn Ruzsinszky
Department of Physics and Quantum Theory Group, Tulane University, New Orleans, Louisiana 70118, USA

(Received 16 June 2012; accepted 20 July 2012; published online 2 August 2012)

We study for the first time the effect of the dependence of meta generalized gradient approximation (MGGA) for the exchange-correlation energy on its input, the kinetic energy density, through the dimensionless inhomogeneity parameter, α, that characterizes the extent of orbital overlap. This leads to a simple MGGA exchange functional, which interpolates between the single-orbital regime, where $\alpha = 0$, and the slowly varying density regime, where $\alpha \approx 1$, and then extrapolates to $\alpha \to \infty$. When combined with a variant of the Perdew-Burke-Ernzerhof GGA correlation, the resulting MGGA performs equally well for atoms, molecules, surfaces, and solids. © *2012 American Institute of Physics*. [http://dx.doi.org/10.1063/1.4742312]

In Kohn-Sham (KS) density functional theory (DFT),[1] the exchange-correlation energy $E_{\rm xc}$ as a functional of the electron spin densities $n_\uparrow(\mathbf{r})$ and $n_\downarrow(\mathbf{r})$ must be approximated. Semilocal approximations (e.g., Refs. 2–7) of the form

$$E_{\rm xc}[n_\uparrow, n_\downarrow] = \int d^3r n\epsilon_{\rm xc}(n_\uparrow, n_\downarrow, \nabla n_\uparrow, \nabla n_\downarrow, \tau_\uparrow, \tau_\downarrow) \qquad (1)$$

require only a single integral over real space and so are practical even for large molecules or unit cells. In Eq. (1), $\nabla n_{\uparrow,\downarrow}$ are the local gradients of the spin densities, $\tau_{\uparrow,\downarrow} = \sum_k |\nabla\psi_{k\uparrow,\downarrow}|^2/2$ the kinetic energy densities of the occupied KS orbitals $\psi_{k\sigma}$ of spin σ, and $\epsilon_{\rm xc}$ the approximate exchange-correlation energy per electron. All equations are in Hartee atomic units. In addition to the spin densities $n_\uparrow$ and $n_\downarrow$ and their gradients, meta generalized gradient approximation (MGGA) includes the kinetic energy density. It can be used, as in the revised Tao-Perdew-Staroverov-Scuseria (revTPSS) MGGA,[6] to distinguish the single-orbital regions from the orbital-overlap regions. However, the dependence of MGGAs on the kinetic energy density is understood much less than that on the density gradient, which MGGA inherits from GGA.[4,5] Such understanding is highly significant for the construction of not only MGGAs theirselves but also fully nonlocal approximations that are based on MGGAs. Therefore, having this insight could be helpful in expediting the shift in DFT from the dominant GGAs to the generally more accurate and computationally comparable MGGAs.[6,8] Here we show the importance and effect of the τ-dependence, leading to a new MGGA that respects a tight Lieb-Oxford bound[9,10] and performs equally well for atoms, molecules, surfaces, and solids.

The semilocal exchange energy of a spin-unpolarized density can be written as

$$E_x^{\rm sl}[n] = \int d^3r n\epsilon_x^{\rm unif}(n)F_x(p,\alpha). \qquad (2)$$

Here, $\epsilon_x^{\rm unif}(n) = -\frac{3}{4\pi}(\frac{9\pi}{4})^{1/3}/r_s$ is the exchange energy per particle of a uniform electron gas (UEG) with $r_s = (4\pi n/3)^{-1/3}$, $p = |\nabla n|^2/[4(3\pi^2)^{2/3}n^{8/3}] = s^2$, and $\alpha = (\tau - \tau^W)/\tau^{\rm unif}$. $\tau = \sum_\sigma \tau_\sigma$, $\tau^W = \frac{1}{8}|\nabla n|^2/n$ is the von Weizsäcker kinetic energy density and $\tau^{\rm unif} = \frac{3}{10}(3\pi^2)^{2/3}n^{5/3}$ is the kinetic energy density of the UEG. τ^W underbounds τ with $\tau^W = \tau$ only for a single-orbital region.[11] Therefore, $\alpha \geq 0$ measures locally how far $n(\mathbf{r})$ deviates from being of a single orbital at the scale of the UEG, and thus characterizes the extent of orbital overlap. The expression for the spin-polarized case follows from exact spin scaling.[12]

In a GGA, the enhancement factor F_x is α-independent and often is monotonically increasing with s, e.g., as in Perdew-Burke-Ernzerhof (PBE),[4] or is increasing for a large range of s.[13–15] This behavior favors less compact systems than does local spin density approximation (LSDA) (e.g., lowering the energy of a set of isolated atoms relative to that of a corresponding molecules, or lowering a surface energy, or enlarging lattice constants). The revTPSS MGGA includes the added ingredient α. It recovers the exact exchange energy of the ground state density of the hydrogen atom and the finiteness of the exchange potential at nuclei, where $\alpha = 0$ (single-orbital regime). Then, at $\alpha \approx 1$ (slowly varying density regime), it restores the second order gradient expansion for a wide range of density and further recovers the fourth order gradient expansion of a slowly varying density. Therefore, the revTPSS enhancement factor is thought to be accurate for small s around $\alpha \approx 1$. However, in the construction of revTPSS, there is no other constraint to guide the functional behavior from $\alpha = 0$ to $\alpha \approx 1$. revTPSS also has an order-of-limits problem[16,17]—the enhancement factor has different values when different sequences of the limits $s \to 0$ and $\alpha \to 0$ are taken, as shown in Fig. 1(a).

Here, we propose a simple exchange enhancement factor that disentangles α and p by a means of a separability assumption,

$$F_x^{\rm int}(p,\alpha) = F_x^1(p) + f(\alpha)[F_x^0(p) - F_x^1(p)], \qquad (3)$$

where $F_x^1(p) = F_x^{\rm int}(p,\alpha=1) = 1 + \kappa - \kappa/(1 + \mu^{\rm GE}p/\kappa)$ and $F_x^0(p) = F_x^{\rm int}(p,\alpha=0) = 1 + \kappa - \kappa/(1 + (\mu^{\rm GE}p + c)/\kappa)$. $F_x^{\rm int}(p,\alpha)$ interpolates between $F_x^0(p)$ and $F_x^1(p)$ through $f(\alpha) = (1-\alpha^2)^3/(1+\alpha^3+\alpha^6)$, which is chosen to guarantee for the functional the second order gradient

expansion, good exchange jellium surface energies, and the Hartree-Fock exchange energy of the 12-noninteracting-electron hydrogenic anion with nuclear charge $Z = 1$ (Ref. 18) ($1s^2 2s^2 2p^6 3s^2$; in the following discussions, $Z = 1$ and electrons are noninteracting in hydrogenic anions if not mentioned otherwise). For a slowly varying density where $\alpha \approx 1$, the second term of the right hand side of Eq. (3) is negligible and of order ∇^6. $F_x^{\rm int}(p,\alpha)$ then reduces to $F_x^1(p)$, which recovers the second order gradient expansion with the first principle coefficient $\mu^{\rm GE} = 10/81$ (Ref. 19) as in PBEsol.[5] $c = 0.28771$ and $\kappa = 0.29$ are two parameters fixed by the exchange energies of the hydrogen atom where $\alpha = 0$ and the 12-electron hydrogenic anion which is used to guide the functional from $\alpha = 0$ to $\alpha \approx 1$. This parameterization also delivers excellent exchange energies for other hydrogenic anions (see Ref. 20). No point in the (c, κ) parameter space could be found without violating the standard Lieb-Oxford bound[9] (i.e., $\kappa \le \kappa^{LO} = 0.804$ (Ref. 4)) if we used a spin-unpolarized hydrogenic anion with electron count below 12. The value, $\kappa = 0.29$, from the 12-electron anion corresponds to a tight Lieb-Oxford bound and a very flat $F_x^0(p)$; see Fig. 1(b). The resulting small derivative at nuclei, $\frac{dF_x^{\rm int}(p,\alpha=0)}{ds}|_{s=0.376} = 0.022$, comes close to satisfying the finiteness constraint on the exchange potential at nuclei. See Ref. 20 for the derivatives of $F_x^{\rm int}(p,\alpha)$.

Compared to revTPSS, the much simpler form, Eq. (3) does not have the order-of-limits problem, though it recovers revTPSS behavior in regions of small s around $\alpha \approx 1$; see Fig. 1(a). In the following discussion, we combine this exchange functional with the variant of the PBE correlation (denoted as vPBEc), in which $\beta(r_s) = 0.066725(1 + 0.1r_s)/(1 + 0.1778r_s)$ as used in revTPSS.[6] The resulting MGGA respects a tight Lieb-Oxford bound with $F_{\rm xc} \le 2.137$, while the standard Lieb-Oxford bound is 2.273.[9,10]

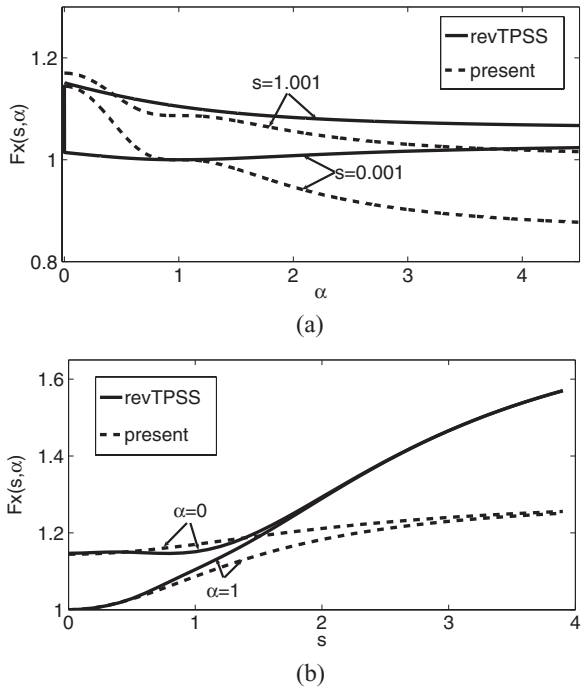

FIG. 1. Exchange enhancement factors vs. α (a) and s (b).

From experience with GGAs,[4,5] we know that the faster an enhancement factor grows with s, the more the functional will favor less compact systems. Since the enhancement factor of the present exchange functional as shown in Fig. 1(b) is largely depressed for a large range of s compared to that of revTPSS, it then seems to be a reasonable extrapolation from experience that the present exchange functional with vPBEc would err toward small lattice constants for solids and high atomization energies for molecules. However, our results (below) show a different scenario. The new MGGA performs equally well for atoms, molecules, surfaces, and solids. The seeming contradiction between performance and expectation is resolved by considering the α-dependence shown in Fig. 1(a). In previous constructions and analysis of MGGAs,[6,8] it is emphasized that α enables MGGAs to distinguish the single-orbital regions from the orbital-overlap regions. Here, we see that the monotonically decreasing dependence of an enhancement factor on α (i.e., the more deviation from being of a single orbital, the less enhancement for the exchange functional) is qualitatively equivalent to monotonically increasing s-dependence, which explains the seeming contradiction as rationalized by the following two observations.

The first observation concerns the changes in s and α distributions from the 10-electron hydrogenic anion ($1s^2 2s^2 2p^6$) to the 12-electron one ($1s^2 2s^2 2p^6 3s^2$),[18] and on the correlation between the changes. Note that these two densities are spherically symmetric. Fig. 2 shows the s and α distributions of these two densities. The shell structure is easily recognized and roughly identified with $\alpha < 1$ for shell regions, which deviate from being of a single orbital less than intershell regions identified with $\alpha > 1$. We can tolerate the confusion caused by this definition for the tail regions, where α could be 0 or $\gg 1$ as shown in Fig. 2, since the tail regions are energetically less important. When an electron is in the intershell region, and α is large even where s is small, the electron's exchange hole is probably not centered close to the electron, but is spread out over the smaller inner shell and the larger outer shell. This spreading of the hole will make the exchange energy density in the intershell region less negative than it would be for a slowly varying or uniform density. One can imagine $F_x < 1$, as can happen in the present exchange functional for small s and large α that is shown in Figs. 1(a) and 2.

When two 3s hydrogenic electrons are added to the 10-electron hydrogenic anion, part of the outermost shell region

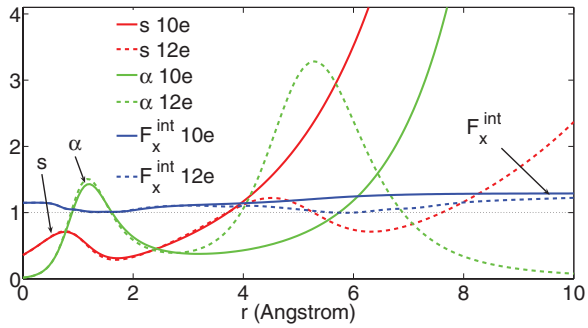

FIG. 2. The s, α, and $F_x^{\rm int}$ distributions for the 10- and 12-electron hydrogenic anions. The line $y = 1$ is plotted to help roughly identify the shell ($\alpha < 1$) and intershell ($\alpha > 1$) regions.

($\alpha < 1$) changes into the intershell region ($\alpha > 1$), which is associated with a decrease of s. Although it is not certain that an increase of α is always associated with a decrease of s during the formation of the intershell of an atom, it is plausible for the intershell region between the outermost core and the valence of an atom within a solid, an important region for determining the lattice constants of solids[21,22] (see second observation). Then, the supposed correlation between s and α in the intershell regions of a solid suggests that monotonically decreasing α-dependence of an enhancement factor has qualitatively the same effect as monotonically increasing s-dependence does for these regions.

The second observation concerns the variations of the lattice constants of the set of 20 solids (SL20) (Ref. 23) and the atomization energies of the AE6 molecule set[24] in response to changes of the α dependence of the enhancement factor. To show the dramatic structural and thermochemical effects and to deduce their origin, $f(\alpha)$ is compared to two variants. The first is $f^{\,0}(\alpha) = 0$, which actually is the PBEsol GGA but with different κ and $\beta(r_s)$. The second one is $f^{\star}(\alpha) = f(\alpha)^{*}h(\alpha)$ with $h(\alpha) = 2/[e^{(\alpha-1)/\gamma} + 1] - 1$. $h(\alpha)$ is equal to 1 for $\alpha < 1$ and to –1 for $\alpha > 1$, respectively, if $\gamma \to 0$. Here, we choose $\gamma = 0.1$ for numerical reasons. Compared to $f(\alpha)$, $f^{\star}(\alpha)$ flips the α dependence for $\alpha > 1$ from monotonically decreasing to monotonically increasing, and therefore favors more the regions with $\alpha > 1$. The choice of the demarcation point at $\alpha = 1$ is natural in view of the first observation and because it helps to satisfy the second order gradient expansion. $f(\alpha)$ and the two variants—whose curves as functions of α are given in Ref. 20—result in three different enhancement factors, $F_x^{\rm int}$, $F_x^{0\rm int}$, and $F_x^{\star\rm int}$.

Table I shows the mean error (ME) and the mean absolute error (MAE) of the lattice constants of the SL20 set,[23] and the AE6 (Ref. 24) atomization energies from LSDA, PBEsol, and variants of $F_x^{\rm int}$. The alleviation, from LSDA to $F_x^{0\rm int}$ and then to $F_x^{\rm int}$, of the overestimation in the atomization energies and of the underestimation in the lattice constants, suggests that the built-in monotonically increasing s-dependence and monotonically decreasing α-dependence in the enhancement factors reduce the preference of LSDA towards compact systems. However, from $F_x^{\rm int}$ to $F_x^{\star\rm int}$, where only the monotonicity of the α-dependence in the range of $[1, \infty]$ is flipped, the solids in the SL20 set are drastically shrunk to such a surprising degree that the lattice constants of $F_x^{\star\rm int}$ are significantly smaller than even those of LSDA. Since the important region in terms of determining the lattice constant of a solid for a functional has been identified[21,22] to be the intershell region of the constituent atoms between the outermost core and the valence regions, the drastic shrinkage from $F_x^{\rm int}$ to $F_x^{\star\rm int}$ is a strong indication that the shell and intershell regions are associated with $\alpha < 1$ and $\alpha > 1$, respectively. Compressing a solid turns part of the outermost core and the valence regions ($\alpha < 1$) into intershell regions ($\alpha > 1$) between them, which $F_x^{\star\rm int}$ favors more than $F_x^{\rm int}$ does. The absence of the monotonically decreasing α-dependence in $F_x^{0\rm int}$, leading to the shrinkage of the solids, could be compensated by enhancing the monotonically increasing dependence on s, as PBEsol does by using κ^{LO}. This implies a decrease of s during the formation of the intershell regions and thus corroborates the correlation between s and α during the formation of the intershell region observed in Fig. 2. Therefore, in $F_x^{\rm int}$, both the monotonically increasing s-dependence and the monotonically decreasing α-dependence have the effect of penalizing the formation of the intershell regions and enlarging the lattice constants. Similar deterioration is also found for the atomization energies of the AE6 set for $F_x^{\star\rm int}$ compared to $F_x^{\rm int}$. Unlike for solids, $F_x^{\star\rm int}$ still significantly improves the AE6 atomization energies over $F_x^{0\rm int}$, and thus LSDA, suggesting that the α-dependence in the range of [0, 1] has stronger influence in atoms and molecules than in solids. Remarkably, the monotonically decreasing α-dependence used in $F_x^{\rm int}$ significantly improves the overestimated AE6 atomization energies from $F_x^{0\rm int}$ to an excellent MAE, 5.4 kcal/mol. This implies that monotonically decreasing α-dependence is in general able to make a functional favor less compact systems, as does monotonically increasing s-dependence.

Now turn to the results for atoms, molecules, surfaces, and solids, which are summarized briefly in Table II in terms of the ME and MAE, or their relative analogs MRE and

TABLE I. Error statistics of lattice constants (Å) of the SL20 solids[23] and atomization energies (kcal/mol) of the AE6 set.[24] See the text for the definitions of F_x^{0int}, $F_x^{\star\rm int}$, and $F_x^{\rm int}$.

		LSDA	PBEsol	$F_x^{0\rm int}$	$F_x^{\star\rm int}$	$F_x^{\rm int}$
	ME	−0.081	−0.012	−0.079	−0.126	0.016
SL20	MAE	0.081	0.036	0.079	0.126	0.023
	ME	77.4	35.9	55.1	22.0	0.6
AE6	MAE	77.4	35.9	55.1	22.6	5.5

TABLE II. Error statistics for various density functionals. The LSDA and PBE enthalpies of formation are from Ref. 6. The lattice constants for M06L are from Ref. 25, where 18 solids, mostly overlapping with the SL20 set, were tested.

	LSDA	PBE	M06L	revTPSS	Present
Exchange energies (Ha) of rare gas atoms					
ME	2.274	0.219	0.204	0.291	0.068
MAE	2.274	0.219	0.210	0.293	0.111
Atomization energies (kcal/mol) of the AE6 molecules					
ME	77.4	12.4	3.2	3.3	0.6
MAE	77.4	15.5	4.2	5.9	5.5
Dissociation energies (kcal/mol) of the W6 water clusters					
ME	5.2	0.0	−0.2	−1.0	0.0
MAE	5.2	0.3	0.4	1.0	0.1
Enthalpies of formation (kcal/mol) of the G3 molecules					
ME	−121.9	−21.7	−1.6	−3.6	−1.6
MAE	121.9	22.2	5.2	4.8	8.3
Jellium surface exchange energies (%)					
MRE	45.8	−20.9	−75.9	−1.0	−7.3
MARE	45.8	20.9	75.9	2.2	8.0
Jellium surface exchange-correlation energies (%)					
MRE	−0.4	−3.1	24.5	2.6	−0.3
MARE	0.4	3.1	24.5	2.6	1.6
Lattice constants (Å) of the SL20 solids					
ME	−0.081	0.051	0.015[a]	0.015	0.016
MAE	0.081	0.059	0.071[a]	0.033	0.023

[a]Reference 25.

MARE. See Ref. 20 for full details. Table II shows that the use of the exact exchange energy of the 12-electron hydrogenic anion guarantees excellent exchange energies for atoms, resulting in good atomization energies for this simple functional. In all categories shown in Table II, the present functional outperforms the standard PBE GGA (PBE is slightly better than the present functional for the cohesive energies of the 20 SL20 solids as shown in Ref. 20). Within the MGGA level, the heavily parameterized M06L (Ref. 7) predicts excellent atomization energies and dissociation energies for the W6 set, at which it aims during the construction. However, it is significantly wrong for the jellium surface energies contributed from the exchange and correlation terms, separately or together. The too-large M06L jellium surface exchange-correlation energies imply that metal bulks are overstabilized, consistent with the too-small lattice constants of main group simple metals, e.g., Na and Al.[25] The present functional and revTPSS are more balanced for different categories and therefore more robust. Compared to revTPSS, the present functional is better for the SL20 solids, comparable for the jellium surface exchange-correlation energies but worse for the exchange part alone, and worse for the G3 molecules. However, the present functional predicts the most accurate dissociation energies of the W6 water clusters among the functionals, implying a good description for the hydrogen bond.

In summary, we have for the first time studied the effect and importance of the dependence of MGGA on the kinetic energy density through the dimensionless inhomogeneity parameter α, and presented a new MGGA exchange functional that disentangles α from the reduced density gradient s by the means of separability assumption. By varying the α-dependence in the exchange functional, we showed that the formation of the intershell region between the outermost core and the valence of an atom within a solid is associated with an increase of α and a decrease of s, suggesting that monotonically decreasing α-dependence of an enhancement factor is qualitatively equivalent to monotonically increasing s-dependence for these intershell regions. The new MGGA that respects this observation is overall comparable in performance, but quite different and much simpler in form, compared to the sophisticated revTPSS MGGA, and thus demonstrates the flexibility and the rich structure of MGGA brought by the extra ingredient of the kinetic energy density.

J.S. thanks John P. Perdew, Gábor I. Csonka, and Stephen E. Glindmeyer for helpful discussions. J.S. and B.X. are supported by National Science Foundation (NSF) under Grant No. DMR08-54769 and A.R. under NSF Cooperative Agreement No. EPS-1003897.

[1] W. Kohn and L. J. Sham, Phys. Rev. **140**, A1133 (1965).
[2] J. P. Perdew and Y. Wang, Phys. Rev. B **45**, 13244 (1992).
[3] J. Sun, J. P. Perdew, and M. Seidl, Phys. Rev. B **81**, 085123 (2010).
[4] J. P. Perdew, K. Burke, and M. Ernzerhof, Phys. Rev. Lett. **77**, 3865 (1996); **78**, 1396 (1997) (Erratum).
[5] J. P. Perdew *et al.*, Phys. Rev. Lett. **100**, 136406 (2008).
[6] J. P. Perdew *et al.*, Phys. Rev. Lett. **103**, 026403 (2009).
[7] Y. Zhao and D. G. Truhlar, J. Chem. Phys. **125**, 194101 (2006).
[8] J. Sun *et al.*, Phys. Rev. B **83**, 121410(R) (2011).
[9] E. H. Lieb and S. Oxford, Int. J. Quantum Chem. **19**, 427 (1981).
[10] M. M. Odashima and K. Capelle, J. Chem. Phys. **127**, 054106 (2007).
[11] S. Kurth, J. P. Perdew, and P. Blaha, Int. J. Quantum Chem. **75**, 889 (1999).
[12] J. P. Perdew *et al.*, Phys. Rev. Lett. **82**, 2544 (1999).
[13] J. P. Perdew *et al.*, Phys. Rev. B **46**, 6671 (1992).
[14] D. J. Lacks and R. G. Gordon, Phys. Rev. A **47**, 4681 (1993).
[15] A. Vela, V. Medel, and S. B. Trickey, J. Chem. Phys. **130**, 244103 (2009).
[16] J. P. Perdew *et al.*, J. Chem. Phys. **120**, 6898 (2004).
[17] A. Ruzsinszky *et al.*, J. Chem. Theory Comput. **8**, 2078 (2012).
[18] V. N. Staroverov *et al.*, Phys. Rev. A **70**, 012502 (2004).
[19] P. R. Antoniewicz and L. Kleinman, Phys. Rev. B **31**, 6779 (1985).
[20] See supplementary material at http://dx.doi.org/10.1063/1.4742312 for the derivatives of the exchange enhancement factor, the table of exchange energies of hydrogenic anions, the figure of $f(\alpha)$ vs. α, and the tables that show details of Tables I and II.
[21] P. Haas *et al.*, Phys. Rev. B **80**, 195109 (2009).
[22] M. Fuchs *et al.*, Phys. Rev. B **57**, 2134 (1998).
[23] J. Sun *et al.*, Phys. Rev. B **84**, 035117 (2011).
[24] B. J. Lynch and D. G. Truhlar, J. Phys. Chem. A **107**, 8996 (2003).
[25] Y. Zhao and D. G. Truhlar, J. Chem. Phys. **128**, 184109 (2008).